J Appl Physiol 128: 838–846, 2020.
First published March 12, 2020; doi:10.1152/japplphysiol.00416.2019.

RESEARCH ARTICLE

Applied mechanical loading to mouse hindlimb acutely increases skeletal perfusion and chronically enhanced vascular porosity

Stephanie Gohin,[1] Behzad Javaheri,[1] Mark Hopkinson,[1] Andrew Anthony Pitsillides,[1] Timothy R. Arnett,[2] and Chantal Chenu[1]

[1]*Department of Comparative Biomedical Sciences, Royal Veterinary College, London, United Kingdom; and* [2]*Department of Cell and Developmental Biology, University College London, London, United Kingdom*

Submitted 19 June 2019; accepted in final form 6 March 2020

Gohin S, Javaheri B, Hopkinson M, Pitsillides AA, Arnett TR, Chenu C. Applied mechanical loading to mouse hindlimb acutely increases skeletal perfusion and chronically enhanced vascular porosity. *J Appl Physiol* 128: 838–846, 2020. First published March 12, 2020; doi:10.1152/japplphysiol.00416.2019.—Blood supply is essential for osteogenesis, yet its relationship to load-related increases in bone mass is poorly defined. Herein, we aim to investigate the link between load-induced osteogenesis and the blood supply (bone perfusion and vascular porosity) using an established osteogenic noninvasive model of axial loading. Accordingly, 12 N mechanical loads were applied to the right tibiae of six male C57BL6 mice at 10–12 wk of age, 3 times/wk for 2 wk. Skeletal perfusion was measured acutely (postloading) and chronically in loaded and contralateral, nonloaded hindlimbs by laser-Doppler imaging. Vascular and lacunar porosity of the cortical bone and tibia load-related changes in trabecular and cortical bone was measured by nanoCT and micro-CT, respectively. We found that the mean skeletal perfusion (loaded: nonloaded limb ratio) increased by 56% immediately following the first loading episode (vs. baseline, $P < 0.01$), and a similar increase was observed after all loading episodes, demonstrating that these acute responses were conserved for 2 wk of loading. Loading failed, however, to engender any significant chronic changes in mean perfusion between the beginning and the end of the experiment. In contrast, 2 wk of loading engendered an increased vascular canal number in the tibial cortical compartment (midshaft) and, as expected, also increased trabecular and cortical bone volumes and modified tibial architecture in the loaded limb. Our results indicate that each episode of loading both generates acute enhancement in skeletal blood perfusion and also stimulates chronic vascular architectural changes in the bone cortices, which coincide with load-induced increases in bone mass.

NEW & NOTEWORTHY This study investigated modifications to the blood supply (bone perfusion and intracortical vascular canals) in mechanoadaptive responses in C57BL6 mice. Each episode of mechanical loading acutely increases skeletal perfusion. Two weeks of mechanical loading increased bone mass and cortical vascular canal number, while there was no chronic increase in hindlimb perfusion. Our findings suggest that the blood supply may participate in the processes that govern load-induced bone formation.

bone architecture; mechanical loading; skeletal perfusion; vasodilation; vascular porosity

INTRODUCTION

Mechanical loading increases bone mass and strength in vivo (12, 25). In contrast, spaceflight, bed rest, hindlimb unloading, and nerve injury are all associated with a reduction in bone loading, leading to decreased bone mineral density (BMD) and strength (1, 11, 52). Exercise and mechanical loading of bone exert a huge influence on bone cell activity by regulating bone interstitial fluid flow, intramedullary pressure, and changes in vasodilation and constriction of blood vessels (35). In addition, blood vessels and bone cells have many ways to communicate, including the production of angiogenic factors, such as vascular endothelial growth factor (VEGF) by osteoblasts (20). However, although bone formation is known to be dependent on both bone blood flow (37) and angiogenesis (6), the links between bone mechanoadaptation and the vascular supply modifications in bone are not completely elucidated.

Repetitive mechanical loading is one of the most robust initiators of osteogenesis, and the effect on bone is evident after only 2 wk of applied loading. Various loading models in rodents have been described and validated previously (12, 30, 50). Using our tibial loading model, we have previously reported that load magnitude greater than 9 N, (3 times/week for 2 wk) enhances cortical and trabecular bone volume (12). Moreover, other studies have shown that the majority of adaptive response in the cortical compartment is at the proximal region, suggesting that the magnitude of mechanoadaptive responses might differ along the length of bone and is spatially coordinated (12, 42, 53).

Bone's adaptive response to loading is dependent on resident bone cells and nutrient supply via the vascular network (35). Previous studies have examined the role of the vascular supply in bone metabolism and reported that a decrease of blood supply to the bone is associated with a reduction of endothelium properties through the principal nutrient artery (PNA), of bone material properties and bone loss during aging (5, 36). Hypoxia has a direct effect on osteoclast (increase in bone resorption) and osteoblast functions (abolition of bone formation) in vitro (3, 51). In addition, cardiovascular disorders (e.g., hypertension) are correlated with a reduction in BMD in women (49) and antihypertensive drugs, such as thiazides, can prevent osteoporotic fractures (4). Moreover, intermittent parathyroid hormone (iPTH) treatment in mice is correlated with an enhanced bone blood flow and bone formation (17) and with increases in blood vessel number and volume (38).

Address for correspondence: C. Chenu, Dept. of Comparative Biomedical Sciences, Royal Veterinary College, London NW1 0TU, UK (email: cchenu@rvc.ac.uk).

Changes in vascularization in response to loading have been poorly studied. One study that focused on intramedullary vessels only showed that 5 wk of treadmill exercise increased vessel number along with enhanced bone formation rate and decreased resorption in secondary spongiosa of the tibia (54). Others have shown that the bone vascularity is enhanced at specific sites of bone formation in response to damaging fatigue loading of the rat ulna (27). Physical exercise in humans and animals affects angiogenesis in vitro and in silico models (16, 26). The links between osteoblasts and endothelial cells after mechanical loading have been extensively studied in these models. For example, the response of MC3T3-E1 osteoblast-like cells to mechanical stimulation induced by an orbital shaker system involves the release proangiogenic factors that are sufficient to increase endothelial cell proliferation, migration and sprouting (26). Moreover, the major angiogenic factor, VEGF, is released from osteoblasts in response to load-induced mechanical stimulation (43). Previous work has also shown that skeletal blood flow in the rat hindlimb measured by radiolabeled microspheres is increased during exercise (41) and following fatigue loading (31). No effect of acute exercise on bone blood flow in dogs during graded treadmill exercise was, however, demonstrated (32). Furthermore, an increase in bone endothelial function in the femoral PNA has been associated with enhanced trabecular bone volume after endurance treadmill training in rats (13). The transport of vascular tracers via the extravascular fluid flow through the bone in tibial middiaphysis was enhanced by one episode of mechanical loading using a four-point bending device (24). These data emphasize that close links between endothelial and bone cell responses to exercise exist but that their specific relationships in vivo in response to a controlled loading stimulus have not yet been fully elucidated.

The effects of exercise on the vascular supply network and osteogenesis depend on loading conditions, such as stress types and strain magnitudes (45). In some studies, using different types of loading allows the dissociation between lamellar or woven bone formation. It was demonstrated that woven bone formation following stress fracture is associated with an increase in blood flow rate measured by positron emission tomography for 14 days after the damaging forelimb loading episode, but there were no changes in the vascular network after lamellar bone formation (45). In contrast, hindlimb unloading by tail suspension has been associated with decreased bone blood perfusion measured by radiolabeled microspheres and bone loss (10).

Most of these studies have used the injections of radiolabeled microspheres to measure the bone blood flow (2). However, this technique is invasive because of the administration of labeled microspheres into the circulation by arterial catheterization or cardiac injection and requires the destruction of the bone (46). Laser-Doppler imaging (LDI), in contrast, is not invasive and monitors temporal variations and dynamic responses of color code map of blood flow (39), offering the possibility to follow the dynamic response of bone blood flow after each loading episode.

The aim of this study was to use an in vivo model of mechanical loading of the tibia to investigate the dynamic changes in skeletal perfusion after each episode of mechanical loading and to assess the ensuing changes in cortical vascular porosity that are engendered by a 2 wk-long osteogenic/antiresorptive mechanical loading protocol in male C57BL6 mice. We hypothesized that acute changes in bone blood supply and chronic bone vascular microarchitecture will correlate with mechanoadaptive bone mass changes. We make the novel observation that loading leads to enhancement of bone perfusion during the acute period, as well as chronic modifications in the cortical bone vascular network, consistent with the new vascular structures.

MATERIALS AND METHODS

Study design. Six male C57BL/6 mice (10–12 wk of age) were obtained from Charles River Laboratories (UK) and maintained under controlled temperature (21°C) and lighting with 12:12-h light-dark cycle. They received a standard mouse diet and water ad libitum. The body weight of all mice was measured every week.

After 1 wk of acclimation, the right tibiae of each mouse was loaded using a servo-hydraulic material testing machine (model HC10, Dartec, UK), three times a week for 2 wk at 12 N under general anesthesia, as described below. Blood perfusion in both loaded and contralateral, left (control) hindlimbs was monitored weekly, before (baseline) and immediately after mechanical loading using laser-Doppler imaging (LDI) under general anesthesia, as explained below.

At the end of the study, mice were euthanized by cervical dislocation; right and left tibia were dissected, fixed in 4% formaldehyde (Alfa Aesar, Ward Hill, MA) for 24 h, and stored in 70% ethanol for microcomputed tomography (micro-CT) imaging. Following micro-CT scanning, all tibiae were dehydrated in acetone for 48 h and embedded in methyl methacrylate (MMA; Sigma, UK) at low temperature for nanoCT scan. All procedures performed in this study conform to the principles and guidelines established by the Animals Scientific Procedures Act and comply with UK Home Office regulations.

In vivo tibial axial loading. Mice were anesthetized with isoflurane gas (4%) balanced by oxygen approximatively for 10 min. Mechanical loading was applied to the right tibia, as described previously (12). Briefly, axial compressive loads were applied with a maximum peak of 12 N for 0.05 s, with a rise and fall time each of 0.025 s using a servo-hydraulic material testing machine. Right tibiae were loaded three times a week for 2 wk (40 cycles/day). The contralateral leg (left tibia) was, therefore, used as a control.

Measurement of hind limb perfusion using laser-Doppler imaging. Laser-Doppler imaging (MoorLDI2 Imager, Moor Instruments, UK) was used to monitor skeletal perfusion in both loaded and nonloaded hindlimbs. To avoid skin irritation, hair on both thighs of mice was shaved with a depilatory cream 2 days before measuring blood perfusion.

During the experiment, mice were anesthetized with isoflurane gas (2%) balanced by oxygen for approximatively 33–35 min. Body temperature was maintained constant using a heated pad. Bone perfusion was recorded 10 min before the mechanical loading episode (baseline) and immediately after for 30 min (acute effect) under general anesthesia. Recordings were performed after each loading session (six sessions in 2 wk). To assess the chronic changes in bone perfusion after 2 wk of loading, blood perfusion measurements were performed 3 days before the first loading episode (*day 0*) and 3 days after the last loading (*day 17*) under general anesthesia.

The LDI flow meter measures the distribution of blood perfusion (a combination of velocity and concentration of red blood cells) in arbitrary units for a selected region of interest (4.7 cm × 3 cm) with a special resolution of 100 μm/pixel.

The selected region of interest covers tissues from the thigh to the foot to include the tibial artery and vein. The estimated maximum depth of detectable vessels (in soft connective tissues) was 2–3 mm (laser wavelength = 830 nm). The LDI displays a color-coded heat map, where the maximum blood perfusion is indicated in red, and the

less perfused region is indicated in dark blue. Skeletal blood perfusion is expressed as the ratio of perfusion in the loading hind limb versus the nonloaded. We have chosen to illustrate our results by showing blood perfusion ratio between loaded versus nonloaded leg to compensate for the variations among mice, the influence of the sedation, and the changes due to the position of hindlimbs between the loading machine and the LDI during the experiment.

Assessment of bone architecture in tibiae after bone mechanical loading using micro-CT analysis. Right (loaded) and left tibiae (nonloaded) dissected from male C57BL/6 mice were scanned using a high-resolution micro-CT scanner (Skyscan-1172/F Bruker, Kontich, Belgium), achieved at 50 kV, 200 μA, 0.5 mm aluminium filter, and 960-ms integration time. The isotropic voxel size was fixed at 5 μm, the rotation step at 0.6°. Images of the whole tibia were reconstructed using NRecon version 1.6.10.2 (Bruker). Cortical and trabecular compartments were segmented manually and analyzed with CTAn version 1.16.8.0+ (Bruker), as described previously (33). Briefly, the trabecular bone corresponding to 5% of total tibial length starting from 2.5% below secondary spongiosa was analyzed. The standard morphometric parameters evaluated within trabecular compartment were bone volume fraction (BV/TV, computed as the ratio of bone volume, BV, over tissue volume, TV), trabecular thickness (Tb.Th), trabecular separation (Tb.Sp), trabecular number (Tb.N), trabecular pattern factor (Tb.Pf), and structure model index (SMI). The cortical analysis was performed at two locations, 50% of the total tibia length and at the tibiofibular junction in 100 tomograms for both locations. The cortical bone parameters evaluated were tissue area (Tt.Ar), tissue perimeter (Tt.Pm), bone area (Ct.Ar), average cross-sectional cortical thickness (Ct.Th) and mean polar moment of inertia (pMMI). The minimum threshold values for the micro-CT analysis were 60 for trabecular bone and 100 for cortical bone.

Assessment of bone vascular and lacunar canals using nanocomputed tomography. Two regions of tibia were selected for porosity analysis; the tibia midshaft, where adaptive responses were previously reported (12) and the tibiofibular junction, at which no mechanoadaptive responses have been observed (12). These two regions were scanned using Skyscan 1172, with a modified protocol (21): 0.6-μm voxel size, 200 μA, 50 kV, and 5,000-ms exposure time with 0.25-mm aluminium filter (99.999% purity, Goodfellow, Huntington, UK) and 360° at a rotation step of 0.25°. Two-frame averaging was used to remove the signal-to-noise ratio. The scan time for each tibia was ~4 h, and thus, thermal shift correction was employed to reconstruct 300 slices (NRecon 1.6.9; Brucker, Kontich, Belgium). Vascular canals and lacunar pores were discriminated by their size and connectivity, as described previously (29). On the basis of previous studies using confocal and nano-CT (8, 9, 21, 28, 29, 47), pores smaller than 13 μm^3 and larger than 1,500 μm^3 were considered to be noise and vascular porosity, respectively. Morphometric indices for lacunar and vascular canals were determined by measuring the three-dimensional (3D) parameters of each discrete object within the volume of interest after segmentation. These indices for vascular canals included average vascular canal number (N.Ca), vascular canals number per total cortical bone volume (N.Ca/Ct.BV), total vascular canals volume (Ca.Tot.V), and vascular canals volume per total cortical bone volume (Ca.V/Ct.BV). For the lacunar canals, average lacunae number (N.Lc), lacunae number per total cortical bone volume (N.Lc/Ct.BV), lacunae volume (Lc.V), and lacunae volume per total cortical bone volume (Lc.V/Ct.BV) were measured.

Statistical analyses. Sample sizes were determined according to our previous studies (21, 22). Results are reported as the means ± SD. Results for the chronic effect of mean perfusion ratio data at D0 and D17, the bone parameters and cortical porosity (left and right sides) were compared by paired *t*-test. Kinetic mean perfusion ratio data were analyzed by one-way ANOVA, followed by Kruskal-Wallis post hoc test. Statistical analyses were performed using Prism v.7 software (GraphPad, San Diego, CA). The statistical significance threshold was taken as $P < 0.05$.

RESULTS

Applied mechanical loading to tibia induces acute but not chronic increases in hindlimb perfusion. Acute and chronic changes in bone perfusion in both hindlimbs were measured using LDI in mice that exhibited no changes in mean body wt during the 2-wk-long experiment (D0 = 24.1 ± 1.7 g; D17 = 24.5 ± 1.6 g, means ± SD; $n = 6$).

Figure 1 shows the mean perfusion ratio between right (loaded) and left (control) hindlimbs from times before (baseline = 10 min) and after the loading period (recorded for 30 min) for each of the six loading episodes. Before the first loading, the mean perfusion ratio between loaded and nonloaded hindlimbs for the baseline period was 0.977 ± 0.018 a.u., demonstrating that the perfusion in both legs was almost similar. It is evident that the first episode of mechanical loading produced rapid and significant increases in the mean perfusion ratio from 0.977 ± 0.018 to a maximum value of 1.522 ± 0.245 recorded soon just after the loading episode, representing an increase in perfusion of 56% compared with the baseline ($P < 0.01$ vs. baseline; Fig. 1*A*). The second, third, fourth, fifth and sixth episodes of mechanical loading all increased the mean perfusion ratio with elevations of 51%, 48%, 50%, 64% and 50% compared with the baseline, respectively (Fig. 1, *B–F*). The mean perfusion ratio returned to baseline within 10 min after each episode of loading (Fig. 1).

Our results demonstrate that the loaded hindlimbs were transiently more perfused after the loading episode than the nonloaded limbs. This increase in perfusion ratio occurred repeatedly and persisted throughout each loading episode.

Our data also demonstrate that the accumulated effect of 2 wk of mechanical loading did not, however, affect the mean perfusion ratio, since our results show no statistical difference between baseline on *day 0* (1.005 ± 0.045) and *day 17* (1.028 ± 0.103; Fig. 2, *A* and *B*). These data indicate that applied mechanical loading induces acute, but not chronic, increases in hindlimb perfusion 3 days after the last episode of loading in male C57BL/6 mice.

Mechanical loading increases trabecular and cortical bone parameters. Micro-CT was used to examine the effect of 2 wk of loading on trabecular bone mass and architecture. As expected, the right loaded tibia had higher trabecular bone mass, indicated by significantly greater trabecular volume percent (BV/TV: +17%; $P < 0.05$) and trabecular thickness (Tb.Th: +6%; $P < 0.05$) compared with the left nonloaded tibia (Table 1). The trabecular number also tended to be higher in right loaded compared with the left nonloaded tibia, although this did not reach levels of statistical significance ($P = 0.067$; +11%; Table 1). Trabecular separation, trabecular bone pattern factor (which measures bone connectivity), and SMI were, in contrast, not modified by 2 wk of loading (Table 1).

The effects of loading on cortical bone mass and architecture were measured at 50% of the total length of tibia and at the tibiofibular junction. At 50% of total length of tibia, the right loaded tibia showed greater cortical area (+6%; $P < 0.05$, Table 1) and average thickness (+4.5%; $P < 0.05$, Table 1), but no changes in tissue area, tissue perimeter, or mean polar moment of inertia (pMMI) compared with the nonloaded limb (Table 1). However, at the tibiofibular junction, loading did not modify cortical area, tissue area, average thickness, tissue perimeter, or pMMI in the right loaded tibia compared with the

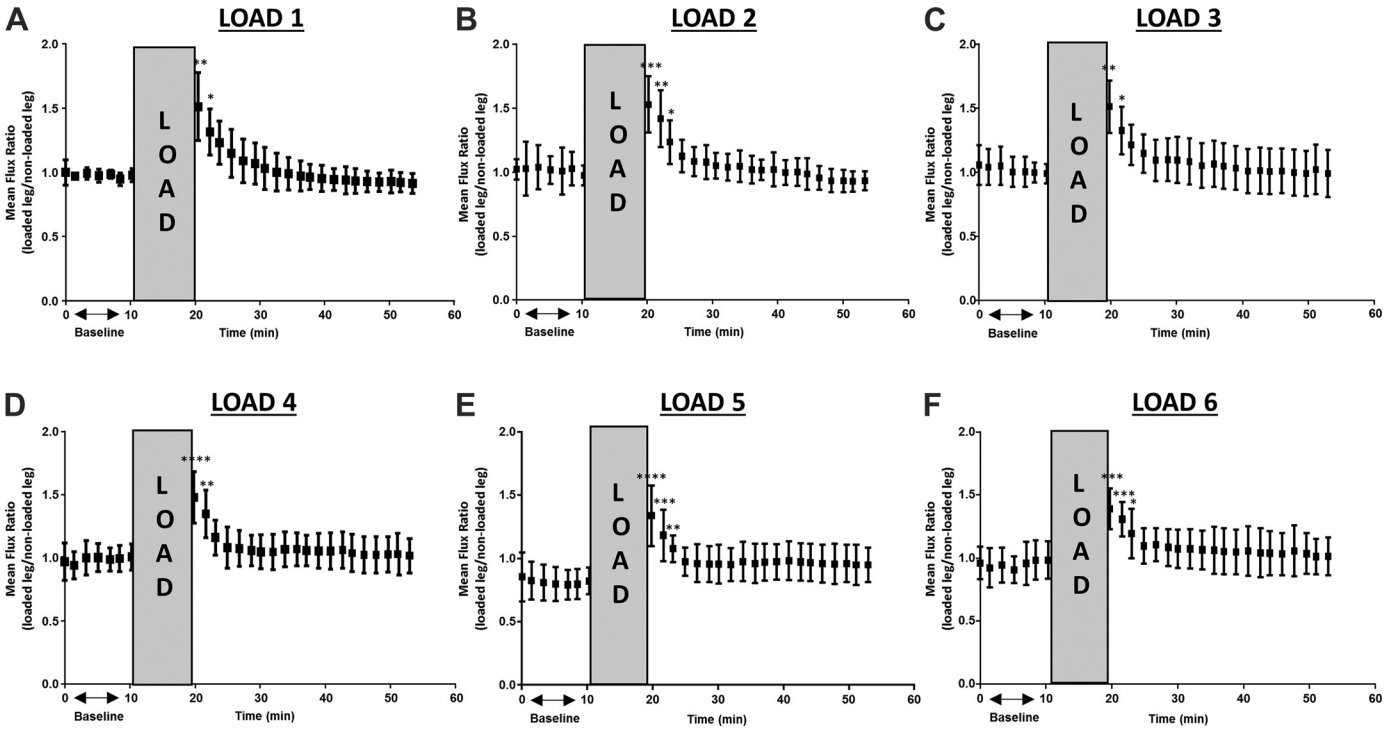

Fig. 1. Mechanical loading increases bone perfusion acutely after each loading episode. Blood perfusion in the loaded and nonloaded legs was evaluated as the ratio of the mean perfusion of the loaded leg to that of the nonloaded one. The mean perfusion ratio was measured after each loading ($n = 6$ mice). *Load 1* (*A*), *Load 2* (*B*), *Load 3* (*C*), *Load 4* (*D*), *Load 5* (*E*), and *Load 6* (*F*). *$P < 0.05$, **$P < 0.01$, ***$P < 0.001$, and ****$P < 0.0001$ vs. baseline. Gray area denotes mechanical loading applied in the right leg for ~10 min.

left nonloaded ones (Table 1). Thus, loading induces a net osteogenic effect at 50% of the tibia length but had no significant effect at the tibiofibular junction.

Load-related cortical bone mass increases at the tibia midshaft are linked to greater vascular but not lacunar porosities. We measured the effects of 2 wk of loading on cortical porosity at both the tibiofibular junction and at 50% of the tibia length using nano-CT. Two weeks of mechanical loading generated raised vascular canals number (+94%; $P < 0.05$, Fig. 3*E*) and greater number when normalized against bone mass (+82%; $P < 0.05$, Fig. 3, *A*, *B*, and *E*) at the tibia midshaft; the total canal volume was not modified (Fig. 3*A*, *B*, and *F*). The number and volume of lacunar pores were also not significantly different in the loaded, compared with the nonloaded, tibiae (Fig. 3*A*, *B*, *G*, and *H*). At the tibiofibular junction, however, neither vascular porosity nor lacunar porosity was different in the loaded versus nonloaded limbs tibia in response to loading (Fig. 3, *C–H*).

DISCUSSION

In this present study, we investigated the role of vascular supply to bone in which osteogenesis had been induced by

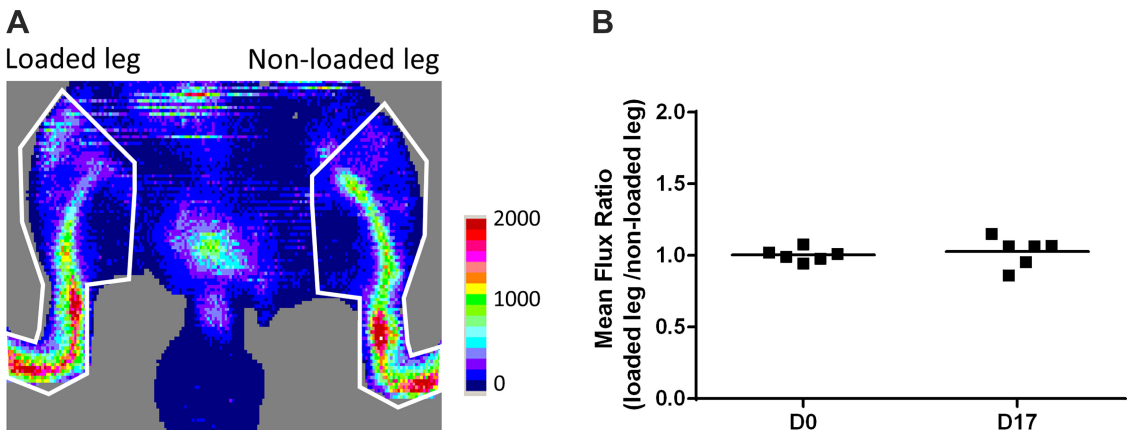

Fig. 2. Lack of effect of chronic mechanical loading on bone perfusion. *A*: representative laser-Doppler image of the mouse hind limb perfusion before 2 wk of mechanical loading (D0). The color-coded heat map shows the maximum (red) and the minimum (blue) levels of perfusion expressed in arbitrary units representing the total blood perfusion. White delimited area is the area used to calculate the mean perfusion ratio (total area: 2 cm^2). *B*: ratio of the mean perfusion in loaded leg to that of the nonloaded one was measured 3 days before the first loading (D0) and 3 days after the last loading (D17) ($n = 6$ mice). $P > 0.05$ vs. D0.

Table 1. *Micro-CT analysis of trabecular and cortical bone at 50% of total length of tibia and tibiofibular junction*

Bone Parameters	Left Nonloaded Tibia	Right Loaded Tibia
	Trabecular Bone Parameters	
BV/TV, %	16.27 ± 2.49	19.03 ± 2.66*
Tb.Th, mm	0.053 ± 0.005	0.057 ± 0.005*
Tb.N, 1/mm	3.05 ± 0.33	3.37 ± 0.51
Tb.Sp, mm	0.17 ± 0.02	0.15 ± 0.04
Tb.Pf, 1/mm	24.21 ± 2.02	28.30 ± 17.55
SMI	2.13 ± 0.16	2.49 ± 1.10

	50% of Total Tibial Length		Tibiofibular Junction	
	Left Nonloaded Tibia	Right Loaded Tibia	Left Nonloaded Tibia	Right Loaded Tibia
	Cortical Bone Parameters			
Tt.Ar, mm^2	1.99 ± 0.23	1.99 ± 0.20	0.95 ± 0.11	0.97 ± 0.12
Ct.Ar, mm^2	0.67 ± 0.06	0.71 ± 0.07*	0.63 ± 0.07	0.65 ± 0.09
Tt.Pm, mm	7.73 ± 0.42	7.63 ± 0.43	6.00 ± 0.37	6.04 ± 0.37
Cs.Th, mm	0.188 ± 0.009	0.196 ± 0.009*	0.206 ± 0.011	0.210 ± 0.017
pMMI, mm^4	0.19 ± 0.04	0.20 ± 0.04	0.13 ± 0.03	0.14 ± 0.04

Both tibia were dissected at the end of the experiment (D17) and analyzed by micro-CT ($n = 6$ mice). Values are means ± SD; *$P < 0.05$ versus left nonloaded tibia. Trabecular parameters: BV/TV, bone volume percent; SMI, structure model index; Tb.N, trabecular number; Tb.Pf, trabecular pattern factor; Tb.Sp, trabecular separation; Tb.Th, trabecular thickness. Cortical parameters: Ct.Ar, bone area; Cs.Th, cross-sectional thickness; pMMI, mean polar moment of inertia; Tt.Ar, tissue area; Tt.Pm, tissue perimeter.

controlled mechanical loading in male C57BL6 mice. We observed an acute and transient increase of bone perfusion in the hindlimb after each episode of loading, which was consistently present after each repeated episode of loading (around 50% of the mean perfusion ratio). We also found, however, that loading did not affect the mean chronic perfusion ratio 3 days after the last episode of loading but did significantly increase the number of vascular canals, and not lacunar porosity, only where enhancement of cortical bone mass is observed.

The new bone formation induced in models of applied mechanical loading is well established. The loading protocol used in our study consists of a multiday loading protocol (three loading episodes/week for 2 wk at 12 N). The design of this study assumes that the bone remodeling induced by mechanical loading in the right leg (loaded leg) does not influence the contralateral bone (nonloaded leg), as previously demonstrated (42). As expected, loading increased trabecular and cortical bone mass and architecture, in agreement with previous studies (12, 42, 53).

The blood flow changes (augmenting or diminishing) result in the neovascularization or vascular rarefaction phenomena and/or vasodilation or vasoconstriction of arteries. At present, the most used bone blood flow measurement techniques in animals are the administration of labeled microspheres (gold standard), the laser-Doppler flowmetry and positron emission tomography (46). A positive correlation between the reference measurement of blood flow (labeled microspheres) and blood perfusion measured by LDI (a continuous and noninvasive measurement of blood flow) supports the use of LDI to measure the velocity of bone blood flow (39). In our study, we used LDI to image skeletal perfusion in the limbs without any dissection of soft tissues to be able to repeat our measurements over time. This is a limitation of our study as we can't be sure to solely quantify bone blood flow. We rather measure limb blood flow. Although LDI has good reproducibility and repeatability, several factors can cause significant variations in blood flow detectable by LDI, such as cardiac activity, temperature, sympathetic activity, anesthesia, and body positioning (18).

Previous measurements of bone blood flow after exercise or applied mechanical loading to bone were mostly performed using labeled microspheres (31, 41, 48). Using LDI, we have found that applied loading produced immediate transient hindlimb perfusion within the 10-min duration of loading. Our results are consistent with other studies using labeled microspheres (31) or ^{18}F-fluoride positron emission tomography (PET) in rats (40) that show that a single period of cyclic fatigue loading immediately increased ulnar blood flow. A major advantage of our study design was the ability in using LDI to assess the immediate skeletal perfusion after each episode of loading longitudinally in the same cohort of mice. Moreover, because our model consists of repeat cycles of loading, we were also able to measure for the first time, the effect of repeat loads on skeletal perfusion. We have demonstrated that this transitory limb bone load-related perfusion persisted during the entire experiment, indicating that the bone vascular response and reactivity did not deteriorate during the application of repeat episodes of loading.

Previous studies have shown differences in the effects of a single period of cycling fatigue loading on bone blood flow depending on load magnitude and frequency. A single period of cyclic compressive fatigue loading using haversine waveform with a very high maximum peak load between 17.3 and 21.4 N for 22,000 cycles increased the bone blood flow for 3 wk, which peaked during the first week postloading (40). In contrast, a similar protocol of fatigue loading (maximum peak load at 16 N, 1,000 cycles) is responsible for an increase in blood flow, persistent only for 5 days (31). In both previous studies, a single and unique bout of fatigue loading was applied with very high force (from 16 N to 21 N) and with a very high number of cycles (from 1,000 cycles to 22,000 cycles). However, in our model of loading, we only observed a vascular transitory effect, as the skeletal perfusion returned to normal, contralateral limb levels within 10 min. This difference might be due to lower load magnitude (12 N) and the number of cycles compared with the aforementioned studies and suggests that the vascular response may depend on the

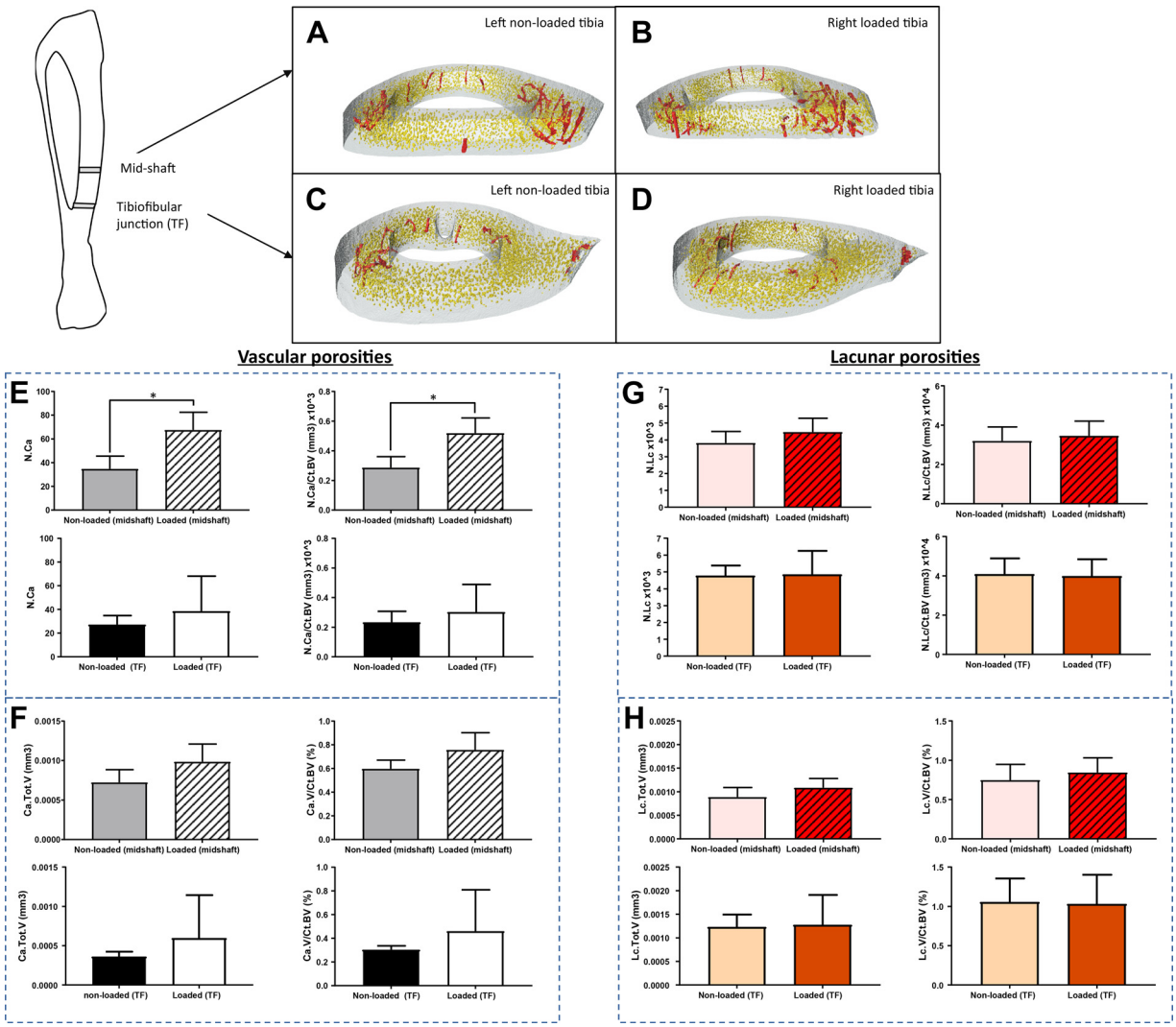

Fig. 3. Mechanical loading increases vascular porosities at the tibia midshaft but not at the tibiofibular junction. Vascular and lacunar porosities were measured at the tibia midshaft and at the tibiofibular junction using nano-computed tomography after 2 wk of mechanical loading. Four representative pictures illustrating vascular canal porosity in red and lacunar porosity in yellow segmented from 300 consecutive images taken *1*) at 50% of total length of tibia in left nonloaded tibia (*A*) and right loaded tibia (*B*) and *2*) at the tibiofibular junction in left nonloaded tibia (*C*) and right loaded tibia (*D*). Bar charts representing average vascular canals number (N.Ca) and vascular canals number per total cortical bone volume (N.Ca/Ct.BV) (*E*), total canal volume (Ca.Tot.V) and vascular canals volume per total cortical bone volume (Ca.V/Ct.BV) (*F*), average lacunae number (N.Lc) and lacunae number per total cortical bone volume (N.Lc/Ct.BV) (*G*), and total lacunae volume (Lc.Tot.V) and lacunae volume per total cortical bone volume (Lc.V/Ct.BV) quantified at the tibia midshaft and at the tibiofibular junction (TF) (*H*). Values are expressed as means ± SD. *$P < 0.05$ vs. left nonloaded tibia. ($n = 4$ mice).

loading protocol. The distinction between our model and the fatigue models used previously may inform our understanding of vascular responses in the context of near-physiological loads, applied in our model, compared with those allied to pathophysiological responses to load-induced fatigue. It is tempting to speculate, therefore, that the vascular responses involved in the fatigue models are more associated with chronic inflammatory responses requiring a longer, more persistent vascular response.

Exercise has been associated with either increases or no changes in bone blood flow (13, 32, 48). It was previously shown that a program of exercise training generates significant improvements in femoral bone properties in old rats via an increase in nitric oxide-mediated vasodilation (13) and improves regional bone and bone marrow blood flow during exercise (41). Treadmill exercise is, however, very different from our in vivo axial loading of bone, as it involves changes in muscle mass, heartbeat rate, blood pressure, and hormone levels. Our model for applying axial loads is more suitable for identifying the modulation of bone adaptation to loading independently of other systemic factors. Our data support the hypothesis that mechanical loading rapidly increases hind-limb perfusion, suggesting direct actions of loading on vascular perfusion that may be mediated by nitric oxide. This is also consistent with our previous work, which has established that bone osteocytes exhibit rapid increases in nitric oxide production in response to mechanical strain (34). This hypothesis needs, however, to be confirmed by future in vivo experiment with the use of nitric oxide synthase (NOS) antagonists or NOS knockout mice.

Hindlimb baseline blood perfusion levels were not modified by any number (up to six) of loading episodes, indicating that

there were no measurable chronic changes in hindlimb baseline blood perfusion after repetitive loading.

Interestingly, before the fifth day of loading, the mean perfusion ratio baseline was below 1, indicating that the baseline blood perfusion of the loaded limb was slightly less than the nonloaded one. It has previously been shown that low- to moderate-intensity treadmill exercise in dogs induces vasoconstriction of bone vessels, while at the same time vasodilation of skeletal muscle vessels (19), suggesting that bones participate in a redistribution of cardiac output during exercise. In our study, the modest decrease in baseline blood perfusion evident before the fifth load suggests that bones have also taken part in a redistribution of newly emerged cardiac output or blood perfusion during loading. Furthermore, the increase in hindlimb perfusion after the fifth episode of loading tended to stay higher than the baseline values, suggesting that the loaded legs may retain the perfusion longer, although this was not significant. A previous study also suggested that the persistence of blood flow elevation for 5 days is potentially correlated with the emerging adaptive responses to loading (31). Furthermore, blood flow elevation is also associated with adaptive bone remodeling in ovariectomised rats (14). Thus, the baseline blood perfusion changes or a new distribution of blood perfusion may appear concomitantly with the adaptive response to loads (new bone formation) in our study.

Chronic exercise is strongly associated with beneficial cardiovascular events and angiogenesis. In this study, we also quantified the cortical vascular network and compared it across two bone regions either lacking (tibiofibular junction) or showing load-related increases in bone mass (midshaft) by nanoCT scanning, to produce true 3D representations of vascular and lacunar porosities (7). We show that loading increases the number of vascular canals but not the lacunar porosities in the region where osteogenic responses are detected. The increase in vascular pores seems to predominate in the anterior portion of the tibial cortex and spread both endocortically and in the subperiosteal surface. Our cross-sectional study does not, however, allow for the identification of newly formed vessels from the preloading status.

Previous work also showed that 2 wk of treadmill training are sufficient in the rat to enhance vessel number in the tibial secondary spongiosa (54). They also demonstrate that 10 days of treadmill training increased VEGF expression in cancellous bone and periosteum. In addition, the bone vascular adaptation induced by 5 wk of training was blocked by anti-VEGF treatment, confirming the important role of angiogenesis in exercise-induced bone gain (54). Furthermore, 2 wk of physical exercise increased bone angiogenesis in tibial secondary spongiosa (vessels number and VEGF expression) coupled with increased cancellous bone formation in running rats (54). Increased osteogenesis induced by fatigue loading was also coupled with increased ulnar vascularity in rats (27). In this paper, the authors demonstrated that the significant enhancement in angiogenesis in the periosteum of loaded ulnae was occurring before the significant increase in bone mass, suggesting that the increase in bone vascularity preceded the increase in bone size (13, 35). Furthermore, bone fatigue loading increased ulnar vascularity only in a specific osteogenic region, similar to our study. The fact that we only observed an increased vascular porosity in the osteogenic region suggests a strong and direct link between the magnitude of the osteogenic response to loading and the number of bone vascular canals. The transient increase in bone perfusion and the observed increase in vascular canals are positively correlated, with the increases in trabecular and cortical bone volume observed in response to loading. Several studies in the literature, indeed, support this hypothesis of a link between bone formation and blood supply (27, 36, 54).

Bones also contain lacuna-canalicular porosity with interconnected fluid-filled pores. The mechanical stimuli induced by the applied loading are detected by osteocytes (23). It is well known that the osteocytes are coupled via the lacunae in the cortical compartment. In our study, two weeks of mechanical loading did not significantly change the lacunar porosity. The lacunar porosity has a lower permeability compared the vascular porosity, and the magnitude of pressure experienced by osteocytes in vivo may reach up to 5 MPa (15). We cannot exclude that the force applied by the loading system in our study is not sufficient to reach the activation of the lacunar porosity. We do not propose either that the vascular effects are independent of osteocytes mechanotransduction. Mechanoadaptive responses in bone are mediated by osteocytes, and while their numbers are not increased, their responses to mechanical stimuli direct osteoblasts to form bones and prevent osteoclast resorption. The culminating effect of this master regulation is new bone formation; increased vasculature is, thus, an inherent component of new bone formation.

In this study, we only measured bone mass/architecture and vascular porosities after 2 wk of loading, but the increase in bone perfusion was visible immediately after the loading episode, as previously shown (46). After stress fracture, the early changes in blood flow occur before angiogenesis that begins at *day 3* during woven bone formation (44). We propose, as previously suggested (13, 34, 35), that the immediate and conserved vasodilation induced by mechanical loading occurs before new vascular structures and osteogenesis, indicating that the increased blood perfusion with the transport of oxygen, nutrients, circulating factors, such as prostaglandins, nitric oxide, and VEGF, and cells initiated the increased cortical vascular porosity and then bone formation.

Conclusion. We report that applied mechanical loading induces bone vascular adaptation, involving acute increases in skeletal perfusion and more long-term elevations in vascular porosity, which are regionally linked to load-related modification in bone mass and architecture. This emphasizes a potential vascular involvement in the osteogenic response induced by 2wk of mechanical loading and that increases in bone blood supply might be a therapeutic target for osteoporosis treatment.

GRANTS

This work was funded by Orthopaedic Research UK (C. Chenu, 516) and Arthritis Research UK (A. Pitsillides, 20581).

DISCLOSURES

No conflicts of interest, financial or otherwise, are declared by the authors.

AUTHOR CONTRIBUTIONS

T.R.A. and C.C. conceived and designed research; S.G. and B.J. performed experiments; S.G., B.J., and M.H. analyzed data; S.G., B.J., A.A.P., and C.C. interpreted results of experiments; S.G. prepared figures; S.G. drafted manuscript; S.G., B.J., M.H., A.A.P., T.R.A., and C.C. edited and revised manuscript; S.G., B.J., M.H., A.A.P., T.R.A., and C.C. approved final version of manuscript.

REFERENCES

1. **Amblard D, Lafage-Proust MH, Laib A, Thomas T, Rüegsegger P, Alexandre C, Vico L.** Tail suspension induces bone loss in skeletally mature mice in the C57BL/6J strain but not in the C3H/HeJ strain. *J Bone Miner Res* 18: 561–569, 2003. doi:10.1359/jbmr.2003.18.3.561.
2. **Anetzberger H, Thein E, Becker M, Zwissler B, Messmer K.** Microspheres accurately predict regional bone blood flow. *Clin Orthop Relat Res* 424: 253–265, 2004. doi:10.1097/01.blo.0000128281.67589.b4.
3. **Arnett TR, Gibbons DC, Utting JC, Orriss IR, Hoebertz A, Rosendaal M, Meghji S.** Hypoxia is a major stimulator of osteoclast formation and bone resorption. *J Cell Physiol* 196: 2–8, 2003. doi:10.1002/jcp.10321.
4. **Aung K, Htay T.** Thiazide diuretics and the risk of hip fracture. *Cochrane Database Syst Rev* (10): CD005185, 2011. doi:10.1002/14651858.CD005185.pub2.
5. **Bloomfield SA, Hogan HA, Delp MD.** Decreases in bone blood flow and bone material properties in aging Fischer-344 rats. *Clin Orthop Relat Res* 396: 248–257, 2002. doi:10.1097/00003086-200203000-00036.
6. **Brandi ML, Collin-Osdoby P.** Vascular biology and the skeleton. *J Bone Miner Res* 21: 183–192, 2006. doi:10.1359/JBMR.050917.
7. **Cardoso L, Fritton SP, Gailani G, Benalla M, Cowin SC.** Advances in assessment of bone porosity, permeability and interstitial fluid flow. *J Biomech* 46: 253–265, 2013. doi:10.1016/j.jbiomech.2012.10.025.
8. **Carriero A, Doube M, Vogt M, Busse B, Zustin J, Levchuk A, Schneider P, Müller R, Shefelbine SJ.** Altered lacunar and vascular porosity in osteogenesis imperfecta mouse bone as revealed by synchrotron tomography contributes to bone fragility. *Bone* 61: 116–124, 2014. doi:10.1016/j.bone.2013.12.020.
9. **Carter Y, Thomas CD, Clement JG, Peele AG, Hannah K, Cooper DM.** Variation in osteocyte lacunar morphology and density in the human femur—a synchrotron radiation micro-CT study. *Bone* 52: 126–132, 2013 [Erratum in *Bone* 54: 179, 2013]. doi:10.1016/j.bone.2012.09.010.
10. **Colleran PN, Wilkerson MK, Bloomfield SA, Suva LJ, Turner RT, Delp MD.** Alterations in skeletal perfusion with simulated microgravity: a possible mechanism for bone remodeling. *J Appl Physiol (1985)* 89: 1046–1054, 2000. doi:10.1152/jappl.2000.89.3.1046.
11. **Collet P, Uebelhart D, Vico L, Moro L, Hartmann D, Roth M, Alexandre C.** Effects of 1- and 6-month spaceflight on bone mass and biochemistry in two humans. *Bone* 20: 547–551, 1997. doi:10.1016/S8756-3282(97)00052-5.
12. **De Souza RL, Matsuura M, Eckstein F, Rawlinson SC, Lanyon LE, Pitsillides AA.** Non-invasive axial loading of mouse tibiae increases cortical bone formation and modifies trabecular organization: a new model to study cortical and cancellous compartments in a single loaded element. *Bone* 37: 810–818, 2005. doi:10.1016/j.bone.2005.07.022.
13. **Dominguez JM II, Prisby RD, Muller-Delp JM, Allen MR, Delp MD.** Increased nitric oxide-mediated vasodilation of bone resistance arteries is associated with increased trabecular bone volume after endurance training in rats. *Bone* 46: 813–819, 2010. doi:10.1016/j.bone.2009.10.029.
14. **Egrise D, Martin D, Neve P, Vienne A, Verhas M, Schoutens A.** Bone blood flow and in vitro proliferation of bone marrow and trabecular bone osteoblast-like cells in ovariectomized rats. *Calcif Tissue Int* 50: 336–341, 1992. doi:10.1007/BF00301631.
15. **Gardinier JD, Townend CW, Jen KP, Wu Q, Duncan RL, Wang L.** In situ permeability measurement of the mammalian lacunar-canalicular system. *Bone* 46: 1075–1081, 2010. doi:10.1016/j.bone.2010.01.371.
16. **Geris L, Vandamme K, Naert I, Vander Sloten J, Van Oosterwyck H, Duyck J.** Mechanical loading affects angiogenesis and osteogenesis in an in vivo bone chamber: a modeling study. *Tissue Eng Part A* 16: 3353–3361, 2010. doi:10.1089/ten.tea.2010.0130.
17. **Gohin S, Carriero A, Chenu C, Pitsillides AA, Arnett TR, Marenzana M.** The anabolic action of intermittent parathyroid hormone on cortical bone depends partly on its ability to induce nitric oxide-mediated vasorelaxation in BALB/c mice. *Cell Biochem Funct* 34: 52–62, 2016. doi:10.1002/cbf.3164.
18. **Greco A, Ragucci M, Liuzzi R, Gargiulo S, Gramanzini M, Coda AR, Albanese S, Mancini M, Salvatore M, Brunetti A.** Repeatability, reproducibility and standardisation of a laser-Doppler imaging technique for the evaluation of normal mouse hindlimb perfusion. *Sensors (Basel)* 13: 500–515, 2012. doi:10.3390/s130100500.
19. **Gross PM, Heistad DD, Marcus ML.** Neurohumoral regulation of blood flow to bones and marrow. *Am J Physiol Heart Circ Physiol* 237: H440–H448, 1979. doi:10.1152/ajpheart.1979.237.4.H440.
20. **Hu K, Olsen BR.** Vascular endothelial growth factor control mechanisms in skeletal growth and repair. *Dev Dyn* 246: 227–234, 2017. doi:10.1002/dvdy.24463.
21. **Javaheri B, Carriero A, Staines KA, Chang YM, Houston DA, Oldknow KJ, Millan JL, Kazeruni BN, Salmon P, Shefelbine S, Farquharson C, Pitsillides AA.** Phospho1 deficiency transiently modifies bone architecture yet produces consistent modification in osteocyte differentiation and vascular porosity with ageing. *Bone* 81: 277–291, 2015. doi:10.1016/j.bone.2015.07.035.
22. **Javaheri B, Carriero A, Wood M, De Souza R, Lee PD, Shefelbine S, Pitsillides AA.** Transient peak-strain matching partially recovers the age-impaired mechanoadaptive cortical bone response. *Sci Rep* 8: 6636, 2018. doi:10.1038/s41598-018-25084-6.
23. **Klein-Nulend J, Bacabac RG, Bakker AD.** Mechanical loading and how it affects bone cells: the role of the osteocyte cytoskeleton in maintaining our skeleton. *Eur Cell Mater* 24: 278–291, 2012. doi:10.22203/eCM.v024a20.
24. **Knothe Tate ML, Steck R, Forwood MR, Niederer P.** In vivo demonstration of load-induced fluid flow in the rat tibia and its potential implications for processes associated with functional adaptation. *J Exp Biol* 203: 2737–2745, 2000.
25. **Lee KC, Maxwell A, Lanyon LE.** Validation of a technique for studying functional adaptation of the mouse ulna in response to mechanical loading. *Bone* 31: 407–412, 2002. doi:10.1016/S8756-3282(02)00842-6.
26. **Liu C, Cui X, Ackermann TM, Flamini V, Chen W, Castillo AB.** Osteoblast-derived paracrine factors regulate angiogenesis in response to mechanical stimulation. *Integr Biol* 8: 785–794, 2016. doi:10.1039/C6IB00070C.
27. **Matsuzaki H, Wohl GR, Novack DV, Lynch JA, Silva MJ.** Damaging fatigue loading stimulates increases in periosteal vascularity at sites of bone formation in the rat ulna. *Calcif Tissue Int* 80: 391–399, 2007. doi:10.1007/s00223-007-9031-3.
28. **McCreadie BR, Hollister SJ, Schaffler MB, Goldstein SA.** Osteocyte lacuna size and shape in women with and without osteoporotic fracture. *J Biomech* 37: 563–572, 2004. doi:10.1016/S0021-9290(03)00287-2.
29. **Mosey H, Núñez JA, Goring A, Clarkin CE, Staines KA, Lee PD, Pitsillides AA, Javaheri B.** *Sost* deficiency does not alter bone's lacunar or vascular porosity in mice. *Front Mater* 4: 27, 2017. doi:10.3389/fmats.2017.00027.
30. **Moustafa A, Sugiyama T, Saxon LK, Zaman G, Sunters A, Armstrong VJ, Javaheri B, Lanyon LE, Price JS.** The mouse fibula as a suitable bone for the study of functional adaptation to mechanical loading. *Bone* 44: 930–935, 2009. doi:10.1016/j.bone.2008.12.026.
31. **Muir P, Sample SJ, Barrett JG, McCarthy J, Vanderby R Jr, Markel MD, Prokuski LJ, Kalscheur VL.** Effect of fatigue loading and associated matrix microdamage on bone blood flow and interstitial fluid flow. *Bone* 40: 948–956, 2007. doi:10.1016/j.bone.2006.11.012.
32. **Pagny JY, Peronnet F, Beliveau L, Sestier F, Nadeau R.** Systemic and regional blood flows during graded treadmill exercise in dogs. *J Physiol (Paris)* 81: 368–373, 1986.
33. **Pereira M, Gohin S, Lund N, Hvid A, Smitham PJ, Oddy MJ, Reichert I, Farlay D, Roux JP, Cleasby ME, Chenu C.** Sclerostin does not play a major role in the pathogenesis of skeletal complications in type 2 diabetes mellitus. *Osteoporos Int* 28: 309–320, 2017. doi:10.1007/s00198-016-3718-0.
34. **Pitsillides AA, Rawlinson SC, Suswillo RF, Bourrin S, Zaman G, Lanyon LE.** Mechanical strain-induced NO production by bone cells: a possible role in adaptive bone (re)modeling? *FASEB J* 9: 1614–1622, 1995. doi:10.1096/fasebj.9.15.8529841.
35. **Prisby RD.** Mechanical, hormonal and metabolic influences on blood vessels, blood flow and bone. *J Endocrinol* 235: R77–R100, 2017. doi:10.1530/JOE-16-0666.
36. **Prisby RD, Ramsey MW, Behnke BJ, Dominguez JM II, Donato AJ, Allen MR, Delp MD.** Aging reduces skeletal blood flow, endothelium-dependent vasodilation, and NO bioavailability in rats. *J Bone Miner Res* 22: 1280–1288, 2007. doi:10.1359/jbmr.070415.
37. **Ramasamy SK, Kusumbe AP, Schiller M, Zeuschner D, Bixel MG, Milia C, Gamrekelashvili J, Limbourg A, Medvinsky A, Santoro MM, Limbourg FP, Adams RH.** Blood flow controls bone vascular function and osteogenesis. *Nat Commun* 7: 13601, 2016. doi:10.1038/ncomms13601.
38. **Roche B, Vanden-Bossche A, Malaval L, Normand M, Jannot M, Chaux R, Vico L, Lafage-Proust MH.** Parathyroid hormone 1-84 targets bone vascular structure and perfusion in mice: impacts of its administra-

tion regimen and of ovariectomy. *J Bone Miner Res* 29: 1608–1618, 2014. doi:10.1002/jbmr.2191.
39. **Shymkiw RC, Zernicke RF, Forrester KR, Bray RC.** Evaluation of laser-Doppler perfusion imaging for measurement of blood flow in cortical bone. *J Appl Physiol (1985)* 90: 1314–1318, 2001. doi:10.1152/jappl.2001.90.4.1314.
40. **Silva MJ, Uthgenannt BA, Rutlin JR, Wohl GR, Lewis JS, Welch MJ.** In vivo skeletal imaging of 18F-fluoride with positron emission tomography reveals damage- and time-dependent responses to fatigue loading in the rat ulna. *Bone* 39: 229–236, 2006. doi:10.1016/j.bone.2006.01.149.
41. **Stabley JN, Moningka NC, Behnke BJ, Delp MD.** Exercise training augments regional bone and marrow blood flow during exercise. *Med Sci Sports Exerc* 46: 2107–2112, 2014. doi:10.1249/MSS.0000000000000342.
42. **Sugiyama T, Price JS, Lanyon LE.** Functional adaptation to mechanical loading in both cortical and cancellous bone is controlled locally and is confined to the loaded bones. *Bone* 46: 314–321, 2010. doi:10.1016/j.bone.2009.08.054.
43. **Thi MM, Suadicani SO, Spray DC.** Fluid flow-induced soluble vascular endothelial growth factor isoforms regulate actin adaptation in osteoblasts. *J Biol Chem* 285: 30931–30941, 2010. doi:10.1074/jbc.M110.114975.
44. **Tomlinson RE, McKenzie JA, Schmieder AH, Wohl GR, Lanza GM, Silva MJ.** Angiogenesis is required for stress fracture healing in rats. *Bone* 52: 212–219, 2013. doi:10.1016/j.bone.2012.09.035.
45. **Tomlinson RE, Shoghi KI, Silva MJ.** Nitric oxide-mediated vasodilation increases blood flow during the early stages of stress fracture healing. *J Appl Physiol (1985)* 116: 416–424, 2014. doi:10.1152/japplphysiol.00957.2013.
46. **Tomlinson RE, Silva MJ.** Skeletal blood flow in bone repair and maintenance. *Bone Res* 1: 311–322, 2013. doi:10.4248/BR201304002.
47. **Tommasini SM, Trinward A, Acerbo AS, De Carlo F, Miller LM, Judex S.** Changes in intracortical microporosities induced by pharmaceutical treatment of osteoporosis as detected by high resolution micro-CT. *Bone* 50: 596–604, 2012. doi:10.1016/j.bone.2011.12.012.
48. **Tøndevold E, Bülow J.** Bone blood flow in conscious dogs at rest and during exercise. *Acta Orthop Scand* 54: 53–57, 1983. doi:10.3109/17453678308992869.
49. **Tsuda K, Nishio I, Masuyama Y.** Bone mineral density in women with essential hypertension. *Am J Hypertens* 14: 704–707, 2001. doi:10.1016/S0895-7061(01)01303-6.
50. **Turner CH, Akhter MP, Raab DM, Kimmel DB, Recker RR.** A noninvasive, in vivo model for studying strain adaptive bone modeling. *Bone* 12: 73–79, 1991. doi:10.1016/8756-3282(91)90003-2.
51. **Utting JC, Robins SP, Brandao-Burch A, Orriss IR, Behar J, Arnett TR.** Hypoxia inhibits the growth, differentiation and bone-forming capacity of rat osteoblasts. *Exp Cell Res* 312: 1693–1702, 2006. doi:10.1016/j.yexcr.2006.02.007.
52. **Voor MJ, Brown EH, Xu Q, Waddell SW, Burden RL Jr, Burke DA, Magnuson DS.** Bone loss following spinal cord injury in a rat model. *J Neurotrauma* 29: 1676–1682, 2012. doi:10.1089/neu.2011.2037.
53. **Yang H, Embry RE, Main RP.** Effects of loading duration and short rest insertion on cancellous and cortical bone adaptation in the mouse tibia. *PLoS One* 12: e0169519, 2017. doi:10.1371/journal.pone.0169519.
54. **Yao Z, Lafage-Proust MH, Plouët J, Bloomfield S, Alexandre C, Vico L.** Increase of both angiogenesis and bone mass in response to exercise depends on VEGF. *J Bone Miner Res* 19: 1471–1480, 2004. doi:10.1359/JBMR.040517.